coatings

MDPI

Article

Experimental Assessment of the Performance of Two Marine Coatings to Curb Biofilm Formation of Microfoulers

Sara I. Faria [1], Rita Teixeira-Santos [1], Luciana C. Gomes [1], Elisabete R. Silva [2,3], João Morais [4], Vítor Vasconcelos [4,5] and Filipe J. M. Mergulhão [1,*]

1 LEPABE—Laboratory for Process Engineering, Environment, Biotechnology and Energy, Faculty of Engineering, University of Porto, Rua Dr. Roberto Frias, 4200-465 Porto, Portugal; sisf@fe.up.pt (S.I.F.); ritadtsantos@fe.up.pt (R.T.-S.); luciana.gomes@fe.up.pt (L.C.G.)
2 BioISI—Biosystems & Integrative Sciences Institute, Departmento de Química e Bioquímica, Faculdade de Ciências, Universidade de Lisboa, Campo Grande, 1749-016 Lisboa, Portugal; ersilva@fc.ul.pt
3 CERENA—Centro de Recursos Naturais e Ambiente, Departamento de Engenharia Civil, Instituto Superior Técnico, Universidade de Lisboa, Avenida Rovisco Pais, 1049-001 Lisboa, Portugal
4 CIIMAR—Interdisciplinar Centre of Marine and Environmental Research, University of Porto, Terminal de Cruzeiros do Porto de Leixões, Avenida General Norton de Matos, S/N, 4450-208 Matosinhos, Portugal; jmorais@ciimar.up.pt (J.M.); vmvascon@fc.up.pt (V.V.)
5 FCUP—Faculty of Sciences, University of Porto, Rua do Campo Alegre, 4069-007 Porto, Portugal
* Correspondence: filipem@fe.up.pt; Tel.: +351-225081668

Received: 31 July 2020; Accepted: 15 September 2020; Published: 18 September 2020

Abstract: Biofilms formed on submerged marine surfaces play a critical role in the fouling process, causing increased fuel consumption, corrosion, and high maintenance costs. Thus, marine biofouling is a major issue and motivates the development of antifouling coatings. In this study, the performance of two commercial marine coatings, a foul-release silicone-based paint (SilRef) and an epoxy resin (EpoRef), was evaluated regarding their abilities to prevent biofilm formation by *Cyanobium* sp. and *Pseudoalteromonas tunicata* (common microfoulers). Biofilms were developed under defined hydrodynamic conditions to simulate marine settings, and the number of biofilm cells, wet weight, and thickness were monitored for 7 weeks. The biofilm structure was analyzed by confocal laser scanning microscopy (CLSM) at the end-point. Results demonstrated that EpoRef surfaces were effective in inhibiting biofilm formation at initial stages (until day 28), while SilRef surfaces showed high efficacy in decreasing biofilm formation during maturation (from day 35 onwards). Wet weight and thickness analysis, as well as CLSM data, indicate that SilRef surfaces were less prone to biofilm formation than EpoRef surfaces. Furthermore, the efficacy of SilRef surfaces may be dependent on the fouling microorganism, while the performance of EpoRef was strongly influenced by a combined effect of surface and microorganism.

Keywords: antifouling coatings; biofilm formation; epoxy resin; marine biofouling; microfoulers; silicone-based paint

1. Introduction

In marine environments, aquatic micro and macroorganisms—such as bacteria, algae, and invertebrates—spontaneously colonize submerged surfaces in a process known as biofouling [1,2]. This natural phenomenon has severe economic and environmental implications all over the world [1–3]. Fouling organisms attached to marine vessel hulls promote surface corrosion and increase frictional drag, leading to higher dry-docking periods and fuel consumption, respectively [1]. Additionally, biofouling can

damage several marine facilities, including oil production platforms, aquaculture systems, and industrial marine water inlet systems, causing substantial economic losses [1]. Furthermore, marine biofouling promotes the bio-invasion of non-indigenous species traveling with marine vessels (ships, yachts, or sailing boats) between different ecosystems, playing a negative impact on global biodiversity [4–6]. Therefore, inhibiting biofouling is one of the most important challenges faced by marine industries and environmental agencies.

The biofouling process begins with the colonization of microfoulers (e.g., cyanobacteria, bacteria, algae, and diatoms) and biofilm formation [7,8]. Biofilms formed on marine surfaces protect microorganisms from the action of adverse environmental conditions and allow the occurrence of macrofouling by bryozoans, mollusks, polychaeta, tunicates, coelenterates, or fungi (marine macrofoulers) [9]. In recent decades, several authors have sought to develop efficient and environmentally friendly marine coatings, aiming to inhibit biofilm formation of microfoulers as a preventive strategy to reduce or delay marine biofouling and its undesirable consequences.

In this study, the performance of two commercial marine coatings—a silicone-based paint (SilRef) and an epoxy resin (EpoRef)—was evaluated to prevent biofilm formation by marine microfoulers. The silicone-based paint is a third-generation hydrogel-based fouling-release coating (FRC), frequently used to coat the ship's hulls, marine water inlet piping, and grids in power stations [10]. It combines hydrogel polymers with silicone fouling-release technology to originate polydimethylsiloxane (PDMS) matrices with self-stratifying hydrogel-promoting polymers, conferring, upon water contact, a more hydrophilic character to the hydrophobic polymer matrix and additives. It is thus able to prevent or weaken hydrophobic or hydrophilic interactions, minimizing the adsorption of proteins, bacteria, and complementing the ability of the original FRC approach [11]. In recent years, FRCs—including PDMS-based matrices—have attracted considerable attention because they are biocide-free and hence environmentally friendly, efficient, and have a relatively long life-cycle [1,8,12]. Silicone polymers have been widely employed in FRC development due to their ability to provide coating films of low surface tension and porosity, excellent elasticity, heat resistance, and durability against UV irradiation [8]; as well as proven efficacy against common marine algae, diatoms, tube worms, hydrozoans, barnacles, and mussels [12,13]. Additionally, among the most used coating materials, hydrogel polymers combined with diverse other polymers have demonstrated high antifouling performance against marine organisms, becoming a focus of increasing interest [14,15]. In turn, the polymeric epoxy resin is commonly used to coat the hulls of small recreational vessels [16,17] due to its unique physical, chemical, and mechanical properties, safety issues, and low cost [18]. Epoxy composites also demonstrated high durability and resistance to fatigue and UV irradiation [19].

Although both commercial coatings are typically used in vessel hulls, the microfoulers' response to these surfaces is not adequately characterized. The present study aims to evaluate the long-time performance of a silicone-based paint and an epoxy resin against biofilm formation by two common microfouling organisms, *Pseudoalteromonas tunicata* and *Cyanobium* sp. LEGE 10375, under defined hydrodynamic conditions in order to predict the antibiofouling response in real marine settings where these surfaces can be used. The fouling behavior of *P. tunicata* has been widely described [20,21] and this organism has become one of the preferred test organisms for surface fouling evaluation. *Cyanobium* spp. is distributed in a wide range of habitats like brackish, marine, and freshwater environments around the planet [22]. Given the fouling potential demonstrated in the current study, it is surprising that only one publication assessed the biofilm formation behavior of a strain from this genus (*Cyanobium* sp. LEGE 06097) in controlled hydrodynamics [23]. To the best of our knowledge, the present study is the first to describe the performance of antifouling marine coatings against *Cyanobium* sp. LEGE 10375. Understanding how antifouling surfaces interact with microfoulers can clarify and help to improve their efficacy, leading to the development of new antifouling coatings to address this challenge.

2. Materials and Methods

2.1. Surface Preparation

Two commercial marine coatings, a silicone-based paint (SilRef) and an epoxy resin (EpoRef) were used in this study. Glass coupons (1 cm × 1 cm; Vidraria Lousada, Lda, Lousada, Portugal) were cleaned and disinfected [23] before being used as a substrate for coating. The silicone-based paint was provided by Hempel A/S (HEMPASIL X3+ 87500, Copenhagen, Denmark) and it is a two-component system obtained from blending a base resin (Hempasil Base 87509) and curing agent (Hempasil Crosslinker 98951) in a ratio of 17.8/2.2 (v/v). SilRef-coated glass surfaces were prepared using conventional brush painting, following the recommendations of the manufacturer: a prior glass coupons coating with a universal tie-coat (base resin XA17-17310 and curing agent XA18-RD003) and a curing step at room temperature (about 23 °C) for 8 h, followed by a second coating with the HEMPASIL system, and curing step at room temperature (about 23 °C) for 24 h. Finally, the cured SilRef-coated glass coupons were sterilized with UV radiation for 30 min before use.

The epoxy resin was produced by HB Química (Matosinhos, Porto, Portugal) and consisted of a mixture of HB Eposurf 2 resin and HB Eposurf hardener in a ratio of 10:3 (v/v) [23]. For the production of EpoRef-coated glass surfaces, 70 µL of epoxy resin was deposited on top of the glass coupons using spin coating (Spin150 Polos^{TM}, Paralab, Porto, Portugal) at 6000 rpm, with increments of 1000 rpm, for 40 s. Then, the surfaces were dried in two steps: (i) 12 h at room temperature (approximately 25 °C), and (ii) 3 h at 60 °C, according to the instructions from the manufacturer [23], and sterilized by using immersion in 70% (v/v) ethanol (VWR International S.A.S., Fontenay-sous-Bois, France) for 20 min. Before the biofilm formation experiments, the initial weight of each coupon was determined.

2.2. Surface Characterization

2.2.1. Atomic Force Microscopy (AFM)

AFM studies were carried out using a PicoPlus scanning probe microscope interfaced with a Picoscan 2500 controller (both from Keysight Technologies, Santa Rosa, CA, USA). Each sample was imaged with a 100 × 100 µm^2 piezo-scanner. The surface roughness was determined in 40 × 40 µm^2 scanned areas in three randomly chosen locations per sample (total of three replicates) at room temperature. The SilRef and EpoRef surfaces were analyzed through contact mode, with a v-shape silicon tip, with a spring constant of 0.085 N/m and 0.284 N/m (AppNano, Mountain View, CA, USA), respectively. The scan speed was set at 1.0 L/s. The WSxM5.0 software (Nanotec Electronica, Feldkirchen, Germany) was used to perform the roughness surface measurements and to obtain the 2D images [24]. The roughness height parameter calculated was the average roughness (R_a).

2.2.2. Static Contact Angle Measurements and Surface Free Energy Estimation

Surface hydrophobicity was evaluated according to the approach developed by Oss et al. [25]. Contact angles were determined at 25 ± 2 °C by the sessile drop method through a contact angle meter (Dataphysics OCA 15 Plus, Filderstadt, Germany) using water, formamide, and α-bromonaphthalene as reference liquids, as fully described by Gomes et al. [26], in three independent assays. In the measurements, the drop size was controlled at 4 µL. For each assay, at least 25 measurements were performed for each material.

2.3. Marine Organisms and Growth Conditions

Pseudoalteromonas tunicata DSM 14096 (DSMZ, Braunschweig, Germany) and *Cyanobium* sp. LEGE 10375 were used in this study because they have been described as early colonizers (microfoulers) of marine surfaces [27,28]. Marine *P. tunicata* was stored at −80 °C in 20% (v/v) glycerol; before experiments, bacteria were spread on the complex marine medium Våatanen Nine Salt Solution (VNSS) prepared according to Holmström et al. [29] and supplemented with 15 g/L agar (VWR

International S.A.S., Fontenay-sous-Bois, France), and incubated at 25 °C for 24 h. Then, an overnight culture (16–18 h) of *P. tunicata* was prepared by transferring colonies from the VNSS agar plate to 150 mL of VNSS broth and incubating at 25 °C, 160 rpm. *Cyanobium* sp. strain was isolated from the intertidal zone, on a marine sponge, collected in October 2010, at São Bartolomeu do Mar beach (41.57378 N 8.798556 W) located in Esposende, Portugal. This cyanobacterial strain belongs to the Blue Biotechnology and Ecotoxicology Culture Collection (LEGE-CC) deposited at the Interdisciplinary Centre of Marine and Environmental Research (CIIMAR), Porto, Portugal [30]. Cyanobacteria were grown in 750 mL Z8 medium supplemented [31] with 25 g/L of synthetic sea salts (Tropic Marin) and B12 vitamin (Sigma Aldrich, Merck, Saint Louis, MO, USA) under 14 h light (10–30 mol photons/m^2/s, λ = 380–700 nm)/10 h dark cycles at 25 °C.

2.4. Biofilm Formation

Biofilm experiments were performed using 12-well microtiter plates (VWR International, Carnaxide, Portugal) under controlled hydrodynamic conditions. Sterilized SilRef and EpoRef coupons were fixed to the microplate wells with double-sided adhesive tape [23]. A *P. tunicata* suspension at an optical density (OD 610 nm) of 0.1 (which corresponds to 10^8 cells/mL) was prepared from an overnight culture, while the cyanobacterial culture was centrifuged to remove any traces of the supplemented Z8 medium and the pellet was resuspended in fresh VNSS medium to a final concentration of 10^8 cell/mL. Subsequently, 3 mL of each cell suspension was added to the wells, and the plates were incubated at 25 °C in an orbital shaker with 25 mm diameter (Agitorb 200ICP, Norconcessus, Ermesinde, Portugal) at 185 rpm under alternate light cycles of 14 h light (10–30 mol photons/m^2/s)/10 h dark. According to previous computational fluid dynamic studies performed by the group [23,32], the selected shaking frequency of 185 rpm produces an average shear rate of 40/s and a maximum of 120/s at the plate bottom, including for instance the shear rate estimated for a ship in a harbor (50/s) [33]. Biofilm formation was monitored for seven weeks (49 days) and sampled every seven days. During the incubation period, the culture medium was replaced twice a week. Three independent biofilm formation experiments (biological replicates) were performed with two technical replicates each (two coupons of SilRef or EpoRef).

2.5. Biofilm Analysis

Every seven days, the culture medium was carefully removed, and the coupons were gently washed with 3 mL of 0.85% (v/v) sterile saline solution to remove loosely attached microorganisms. Two coupons from each experimental condition were analyzed regarding (i) the number of biofilm cells, (ii) biofilm wet weight, and (iii) biofilm thickness. Additionally, the biofilm structure was analyzed at day 49 using confocal laser scanning microscopy (CLSM).

2.5.1. Biofilm Cell Counting and Wet Weight

For cell counting, coupons were taken out of the wells, dipped in 2 mL of 0.85% (v/v) sterile saline solution and vortexed for 3 min at maximum power to release biofilm cells. Then, 10 µL of each cell suspension was placed on each side of a Neubauer chamber and observed in a brightfield microscope (Nikon Eclipse LV100 microscope, Nikon Corporation, Tokyo, Japan).

To assess the wet weight of biofilms, coupons were removed from the wells with a tweezer and weighted on an analytical balance. The biofilm wet weight was determined by the difference between the initial weight of coupon (before inoculation) and the weight measured on the sampling day.

2.5.2. Biofilm Thickness

Biofilm thickness was assessed through optical coherence tomography (OCT) (Thorlabs Ganymede Spectral Domain Optical Coherence Tomography system, Thorlabs GmbH, Dachau, Germany) with a central wavelength of 930 nm. Before biofilms were imaged, the culture medium was carefully removed from the microplate wells, the coupons were gently washed, and the wells were filled with 3 mL of 8.5 g/L sodium chloride sterile solution. Since biofilms are essentially composed of

water [34], the established refractive index was 1.40, close to the refractive index of water (1.33). At each sampling day, a minimum of five different fields of view (2D images) per material and microorganism were analyzed and captured. Image analysis was performed using a routine developed in the Image Processing Toolbox from MATLAB 8.0 and Statistics Toolbox 8.1 (The MathWorks, Inc., Natick, MA, USA), as described by Romeu et al. [35].

2.5.3. Confocal Laser Scanning Microscopy (CLSM)

At day 49, coupons containing the biofilms were removed from the microplates, washed with saline solution, and stained with 6 µM Syto9 (Thermo Fisher Scientific, Waltham, MA, USA)—a green cell-permeant nucleic acid marker—for 10 min at room temperature. Each stained sample was mounted on a microscopic slide and image acquisition was performed using a Leica TCS SP5 II Confocal Laser Scanning Microscope (Leica Microsystems, Wetzlar, Germany). All biofilms were scanned at 400 Hz using a 40× water objective lens (LEICA HCX PL APO CS 40.0×/1.10 WATER UV) with a 488-nm argon laser set at 25% intensity. The emitted fluorescence was recorded within the range of 500–600 nm. A minimum of five stacks of horizontal-plane images (512 × 512 pixels, corresponding to 387.5 µm × 387.5 µm) with a *z*-step of 1 µm were acquired per sample.

Three-dimensional (3D) projections of the biofilms were constructed from the CLSM acquisitions using the "Easy 3D" function of the IMARIS 9.1 software (Bitplane, Zurich, Switzerland). Quantitative structural parameters (biovolume and surface coverage) were extracted from confocal image series with the plug-in COMSTAT2 [36] run in ImageJ 1.48v software [37]. While the biovolume provides an estimate of the biomass in the biofilm ($\mu m^3/\mu m^2$), the surface coverage corresponds to the percentage of surface area covered on the biofilm base.

2.6. Data Analysis

Descriptive statistics were used to calculate the mean and standard deviation for the different biofilm parameters (number of biofilm cells, wet weight, thickness, biovolume, and surface coverage).

Data analysis was performed using the GraphPad Prism® for Windows, version 8 (GraphPad Software, Inc., San Diego, CA, USA). Since the variable distribution was normal, Student's *t*-test was used to compare biofilm formation between the two marine surfaces tested (SilRef and EpoRef) for both *P. tunicata* and *Cyanobium* sp. LEGE 10375 strains. The same statistical test was used to compare the biovolume and surface coverage of *P. tunicata* and *Cyanobium* sp. LEGE 10375 biofilms between the two tested surfaces at the end of the experiment (day 49). Significant results were considered for p-values < 0.1.

In order to ascertain the performance of SilRef and EpoRef marine coatings to curb biofilm formation of main microfoulers, the surface and microorganism influence were estimated for each parameter monitored over time (number of biofilm cells, wet weight, and thickness) and represented in radar charts. Radar charts were split into four quadrants and each one represents the average values obtained in each sampling point (days) for the following assays: *P. tunicata* biofilm formation on SilRef (*Ps*/SilR, top right quadrant); *P. tunicata* biofilm formation on EpoRef (*Ps*/EpoR, bottom right quadrant); *Cyanobium* sp. biofilm formation on EpoRef (*Cya*/EpoR, bottom left quadrant); and *Cyanobium* sp. biofilm formation on SilRef (*Cya*/SilR, top left quadrant). The influence of the microorganism on biofilm development was calculated by subtracting the values obtained for the two microfoulers for both SilRef (*Ps*/SilR vs. *Cya*/SilR) and EpoRef (*Ps*/EpoR vs. *Cya*/EpoR) surfaces, whereas the influence of the surface on biofilm development was determined by subtracting the values obtained for two different surfaces for *P. tunicata* (*Ps*/SilR vs. *Ps*/EpoR) and *Cyanobium* sp. (*Cya*/SilR vs. *Cya*/EpoR) microfoulers. All positive differences were considered as increments resulting from the microorganism or surface effect and represented by a colored area (microorganism effect—orange area; surface effect—red area). The combined effect (blue area) has been plotted whenever the surface effect overlapped the microorganism effect.

3. Results

In this study, the antibiofilm efficacy of two commercial marine coatings, a silicone-based paint (SilRef) and an epoxy resin (EpoRef), was determined through the analysis of *Cyanobium* sp. and *P. tunicata* biofilms developed on SilRef- and EpoRef-coated glass substrates for 49 days under hydrodynamic conditions that mimic the marine environment.

The SilRef and EpoRef surfaces were first analyzed concerning their hydrophobicity and roughness (Table 1). Both water contact angles (θ_w) and degree of hydrophobicity (ΔG) indicated that the SilRef is more hydrophobic than the EpoRef surface ($\theta_{w\ SilRef}$ = 108.4° vs. $\theta_{w\ EpoRef}$ = 69.4°, Figure S1; $\Delta G_{\ SilRef}$ = −55.8 mJ/m^2 vs. $\Delta G_{\ EpoRef}$ = −26.7 mJ/m^2). The surface topography of SilRef and EpoRef surfaces was examined by AFM in contact mode (Figure 1). The topography images revealed that both coatings are homogeneous and very smooth. In fact, the roughness of both surfaces is at a nanoscale, suggesting that there are no features in the surfaces to act as niches for the microfoulers. Nevertheless, the SilRef surface displayed higher roughness with an average value (R_a) of 49.7 nm, in opposition to R_a = 12.9 nm for the EpoRef surface (Table 1).

Table 1. Contact angles with water (θ_w), formamide (θ_F) and α-bromonaphthalene (θ_B), hydrophobicity (ΔG) and roughness (R_a) determined for the SilRef and EpoRef surfaces. Values are presented as means ± standard deviations.

Surface	Contact Angles (°)			Hydrophobicity (mJ/m^2)	Roughness (nm)
	θ_w	θ_F	θ_B	ΔG	R_a
EpoRef	69.4 ± 3.0	56.8 ± 3.0	23.3 ± 2.2	−26.7	12.9 ± 2.9
SilRef	108.4 ± 3.5	104.0 ± 1.9	70.0 ± 2.0	−55.8	49.7 ± 8.3

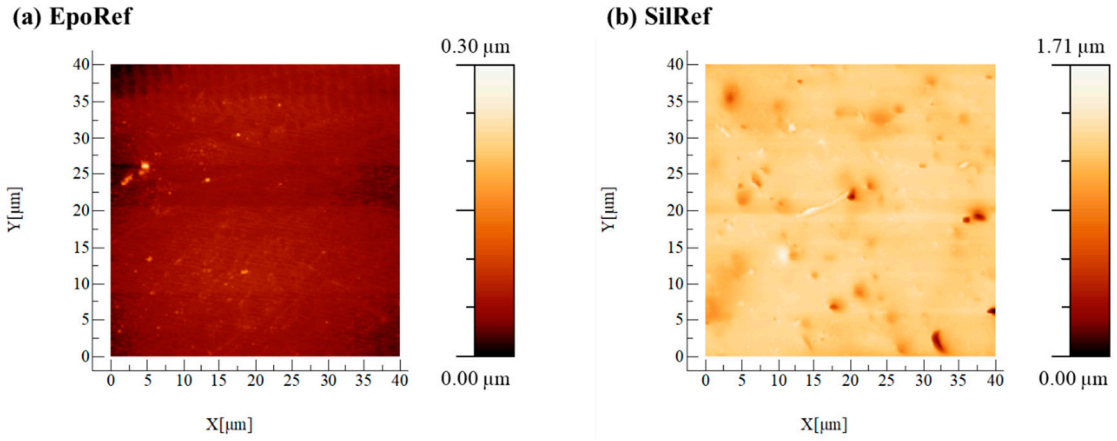

Figure 1. 2D AFM images of EpoRef (**a**) and SilRef (**b**) surfaces with a scan range of 40 µm × 40 µm (contact mode). The color bar corresponds to the *z*-range of the respective image.

Results of biofilm analysis—including the number of biofilm cells, wet weight, and thickness—are presented in Figure 2. In general, regardless of the surface material, the cyanobacterial strain has higher biofilm-forming capacity than *P. tunicata*. This is particularly evident in the last two weeks of the experiment (between days 35 and 49), in which the wet weight and mean thickness values obtained for the cyanobacterial biofilms (Figure 2b,c) were about 26% higher than those of bacterial biofilms (Figure 2e,f). On the other hand, it is possible to globally observe that, while the biofilm parameters for cyanobacteria (in particular, the wet weight and thickness) followed an increasing tendency over time, there was a certain stagnation of the biofilm values for the marine bacteria, regardless of the surface (Figure 2).

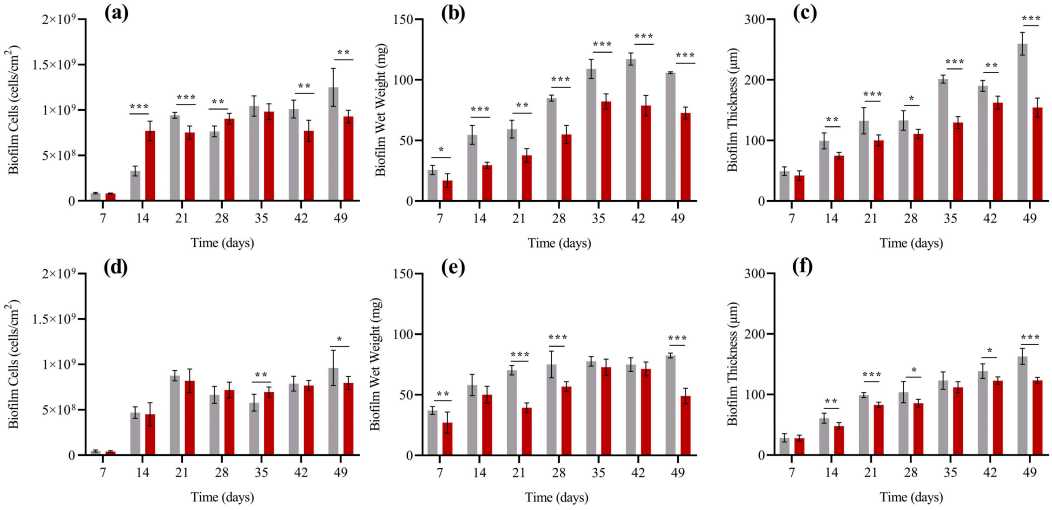

Figure 2. Effect of two commercial coatings (■ EpoRef; ■ SilRef) on biofilm development of *Cyanobium* sp. LEGE 10375 (**a**–**c**) and *Pseudoalteromonas tunicata* (**d**–**f**) for 49 days. The analyzed parameters refer to the number of biofilm cells (**a**,**d**), biofilm wet weight (**b**,**e**), and biofilm thickness (**c**,**f**). Statistical analysis was performed by paired *t*-test, and significant differences between the two surfaces are indicated with *** ($p < 0.01$), ** ($p < 0.05$), and * ($p < 0.1$).

Looking at the cell number of *Cyanobium* sp. biofilms (Figure 2a), there was a growing trend for EpoRef surfaces from day 7 (with 8.39×10^7 cells/cm^2) to the end of the experiment (with 1.25×10^9 cells/cm^2). The beneficial effect of the SilRef surfaces was particularly evident towards the end of the experimental period, when a reduction in the cell number of about 26% was registered compared to EpoRef surfaces for day 49 ($p < 0.05$, Figure 2a). For *P. tunicata* biofilms (Figure 2d), the number of cells increased until day 21 and then kept more or less constant for both surfaces (on average, 7.66×10^8 cells/cm^2). Again, at day 49, the SilRef-coated surfaces presented 17% less cells than the EpoRef surfaces ($p < 0.1$, Figure 2b).

The wet weight of *Cyanobium* sp. biofilms developed either on SilRef or EpoRef surfaces (Figure 2b) increased until day 35. In all sampling points, statistically significant differences were found between the wet weight of biofilms developed on EpoRef and SilRef surfaces. Indeed, on SilRef surfaces, *Cyanobium* sp. biofilms weighted, on average, 33% less than the biofilms formed on EpoRef surfaces. The wet weight of *P. tunicata* biofilms (Figure 2e) increased on both surfaces until day 35 and then remained constant, with exception of biofilms formed on SilRef surfaces whose wet weight decreased on day 49. An average wet weight reduction of 35% was obtained for biofilms developed on SilRef compared to those formed on EpoRef surfaces (Figure 2e).

The mean thickness of *Cyanobium* sp. biofilms generally increased until day 49 (Figure 2c) and biofilms formed on SilRef surfaces had, on average, 27% lower thickness than those developed on EpoRef surfaces throughout the experiment. This difference was particularly visible on day 49, when the biofilm formed on SilRef had almost half the mean thickness of the biofilm grown on EpoRef surfaces ($p < 0.01$, Figure 2c). The thickness of *P. tunicata* biofilms also increased over time (Figure 2f), stabilizing on day 42 for biofilms developed on SilRef surfaces. On average, *P. tunicata* biofilms developed on SilRef surfaces were approximately 15% thinner than those developed on EpoRef surfaces.

The relative importance of surface properties and microorganism type on biofilm formation was estimated for each analyzed parameter (Figure 2) and graphically represented in Figure 3 where only increases in the assayed parameters are depicted. For *Cyanobium* sp. biofilms developed on SilRef surfaces (top left quadrant), the microfouler organism had a strong influence on the increase of biofilm cells, wet weight, and thickness (Figure 3a–c), as represented by the orange area. Additionally, a subtle combined effect was observed between the surface and microorganism (blue area) that contributed to a higher number of cells at an early stage of *Cyanobium* sp. biofilm formation (between day 7 and 28)

(Figure 3a). For *Cyanobium* sp. biofilms formed on EpoRef surfaces (bottom left quadrant), a combined effect between the surface and microorganism (blue area) was responsible for a higher number of biofilm cells, wet weight, and thickness (Figure 3a–c). This effect was more noticeable from day 35 of biofilm formation. Although the microorganism type affected biofilm formation, the combined effect was stronger (blue area > orange area) (Figure 3a–c). Moreover, the surface effect (red area) contributed to an increase of *Cyanobium* sp. biofilm wet weight at an early stage of its development (Figure 3b).

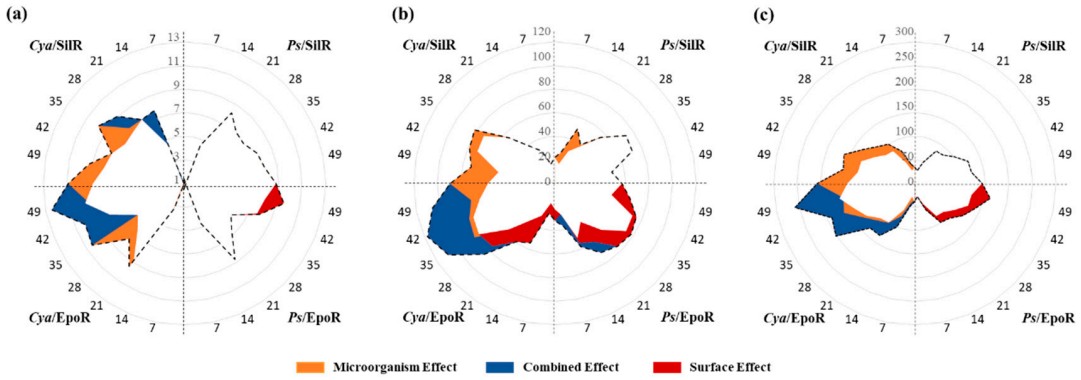

Figure 3. Radar charts representing (**a**) the number of cells (10^8 cells/cm^2), (**b**) wet weight (mg), and (**c**) thickness (μm) for *Pseudoalteromonas tunicata* (*Ps*, right side) and *Cyanobium* sp. LEGE 10375 (*Cya*, left side) biofilms developed on SilRef (upperside) and EpoRef (downside) surfaces. Average values (previously represented in Figure 2) are plotted as a dashed line considering the time scale (days) indicated in each quadrant. The following conditions are depicted in each quadrant: *Ps*/SilR (top right quadrant), *P. tunicata* on SilRef; *Ps*/EpoR (bottom right quadrant), *P. tunicata* on EpoRef; *Cya*/EpoR (bottom left quadrant), *Cyanobium* sp. on EpoRef; *Cya*/SilR (bottom right quadrant), *Cyanobium* sp. on SilRef. Colored areas represent the microorganism or surface effect, which are equivalent to all positive differences observed in each parameter (biofilm cell number, wet weight, and thickness), when subtracting the results obtained at the same microorganism (surface effect) or with the same surface (microorganism effect). Overlap areas are also highlighted, indicating a combined effect of the microorganism and surface.

For *P. tunicata* biofilms formed on SilRef surfaces (top right quadrant), an increase in the assayed parameters is not seen due to the effect of the microorganism type (orange area) as only a slight increase in wet weight can be seen in Figure 3b. In turn, for *P. tunicata* biofilms formed on EpoRef surfaces (bottom right quadrant), a strong influence of the surface (red area) was visible, contributing to a higher number of biofilm cells, wet weight, and thickness (Figure 3a–c). Additionally, the combined effect between the surface and microorganism had a small influence on the biofilm wet weight at an early development stage (days 7 and 14) (Figure 3a).

The structural differences between the *Cyanobium* sp. and *P. tunicata* single-species biofilms formed on the two tested surfaces at the end of the experiment (49 days) were evaluated using CLSM. Examples of 3D biofilm reconstructions are presented in Figure 4. It is possible to observe that denser and thicker biofilms grew on the epoxy resin, regardless of the microorganism (Figure 4a,c), which confirms the results of the biofilm cell number (Figure 2a,b) and thickness (Figure 2c,d) obtained by brightfield microscopy and OCT, respectively. On the contrary, biofilms formed on the silicone-based coating were thinner and did not cover the entire surface area (Figure 4b,d) due to the formation of large cell aggregates, which are particularly visible in the *P. tunicata* biofilm (Figure 4d). In fact, while in the EpoRef surfaces, both *Cyanobium* sp. and *P. tunicata* biofilms displayed a surface coverage above 70%, it was only around 45% in the SilRef surfaces ($p < 0.01$, Figure 5b,d). With regard to biovolumes (Figure 5a,c), they were also significantly higher for the EpoRef surfaces when compared to the SilRef surfaces. In the case of cyanobacteria, the biovolume determined for the EpoRef surfaces was about 3 times higher than that found for the SilRef surfaces after 49 days of biofilm development. This is

correlated to the higher cell density and weight of cyanobacterial biofilms on the EpoRef coating at the experimental end-point (Figure 2a,b).

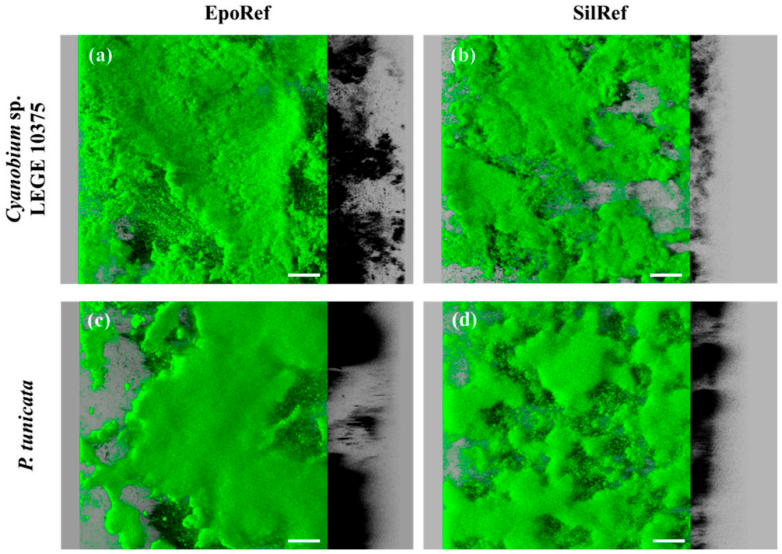

Figure 4. Representative biofilm structures of (**a**) *Cyanobium* sp. LEGE 10375 on EpoRef surface, (**b**) *Cyanobium* sp. LEGE 10375 on SilRef surface, (**c**) *Pseudoalteromonas tunicata* on EpoRef surface, and (**d**) *Pseudoalteromonas tunicata* on SilRef surface after 49 days of biofilm formation. These images were obtained from confocal *z*-stacks using IMARIS software and present an aerial, 3D view of the biofilms (shadow projection on the right). The scale bar is 50 µm.

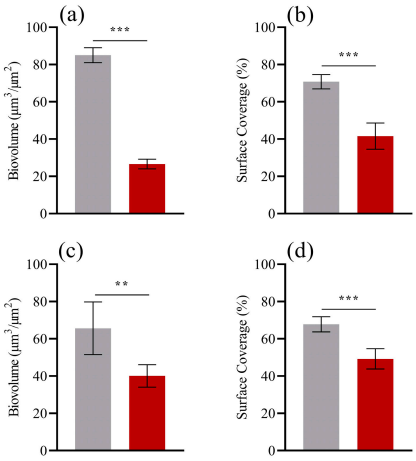

Figure 5. Biofilm structural parameters obtained from the *z*-stacks acquired at the confocal laser scanning microscopy (CLSM) after 49 days: biovolume (**a**,**c**) and surface coverage (**b**,**d**). *Cyanobium* sp. LEGE 10375 (**a**,**b**) and *Pseudoalteromonas tunicata* (**c**,**d**) biofilms formed on EpoRef (■) and SilRef (■) surfaces. Standard deviations for three independent experiments are presented. Statistical analysis was performed by using paired *t*-test, and significant differences between two surfaces are indicated with *** ($p < 0.01$) and ** ($p < 0.05$).

4. Discussion

In this study, the long-term performance of two commercial marine coatings, a silicone-based paint and an epoxy resin, to prevent biofilm formation by common microfoulers was demonstrated through the kinetic evaluation of different biofilm parameters, including the number of biofilm cells, wet weight, and thickness. For this purpose, *Cyanobium* sp. and *P. tunicata* biofilms were developed on both surfaces for seven weeks under controlled hydrodynamic conditions that mimic those found in some marine settings. As the hydrodynamic forces bring a strong impact on marine biofilm

development [23,32,38,39], the experiments were performed under specific shear forces that include the shear rate estimated for a ship in a harbor (50/s) [33] in order to increase the predictive value of the results.

At an initial development stage (until day 28), *Cyanobium* sp. biofilms formed on SilRef-coated surfaces presented, on average, a higher number of cells compared to biofilms formed on EpoRef surfaces. However, from day 35 onwards, the number of biofilm cells stabilized on SilRef surfaces, while on EpoRef surfaces this number increased up to day 49. A similar biofouling response was detected for *P. tunicata* biofilms. Until day 28, the number of cells of biofilms formed on SilRef surfaces was slightly higher than those obtained for biofilms formed on EpoRef. However, on SilRef surfaces, the biofilm cell number was maintained, while on EpoRef surfaces, it increased up to day 49. Based on this parameter, the EpoRef surfaces effectively inhibited biofilm formation at initial stages (until day 28), while SilRef surfaces showed higher antifouling activity during biofilm maturation (from day 35 onwards). Indeed, surface characterization analysis demonstrated that the EpoRef surface is less hydrophobic and rough, which may explain its higher performance at initial stages of biofilm formation. In opposition, the higher hydrophobicity and roughness of SilRef may have hindered their initial antifouling activity. However, despite several studies reporting a correlation between the surface hydrophobicity and roughness and cell attachment [40,41], there is evidence that the biofilm formation induces changes in the surface properties [42,43]. These findings corroborate the higher antifouling activity of SilRef surfaces during the biofilm maturation stages.

SilRef is a commercial coating, and accordingly with its technical properties, is based on a dual-mode of action, a 'non-stick' ability and a foul-release effect, allied to its relative higher elasticity (Young's modulus). These properties may contribute to decreasing fouling settlements and cell cohesion interactions [8,10,33], as confirmed by using confocal microscopy for both studied marine strains. Besides, this dual-action has improved the FRC original properties by the hydrogel contribution in its singular hydrogel-PDMS polymeric matrix, which acquires a more hydrophilic character upon contact with water. Thus, it can prevent either weaker hydrophobic or hydrophilic interactions, which can delay the adsorption of proteins, bacteria, and subsequent fouling [11,12,15].

Recently, Faria et al. demonstrated the impact of the surface properties on marine biofilm formation under controlled hydrodynamic conditions [23]. Indeed, surface properties may promote cell–surface interactions that, even in a low magnitude, may facilitate microfouler retention and contribute to biofilm development [44].

Although there was a shift between the number of cells of biofilms formed on SilRef and EpoRef surfaces that may be dependent on the biofilm age, wet weight and thickness analysis revealed that, in all development stages, *Cyanobium sp.* and *P. tunicata* biofilms formed on SilRef surfaces showed lower weight and were thinner than those developed on EpoRef surfaces. These results should be interpreted considering that a biofilm is an organized community of aggregated cells, living at an interface between a surface and a liquid phase, and embedded in a self-produced organic polymeric matrix [9] whose behavior is driven by cell–cell, cell–extracellular polymer, and cell–surface interactions [45]. As a consequence of these dynamic interactions, biofilm size, matrix composition, architecture, and cellular physiology can change during biofilm development [46,47]. Thus, the discrepancy initially observed between the number of biofilm cells and biofilm weight and thickness may be an indirect effect of the cell–surface interactions. Nevertheless, both biofilm wet weight and thickness analysis also suggested that SilRef-coated surfaces had a better performance in preventing *Cyanobium sp.* and *P. tunicata* biofilm formation than EpoRef surfaces. Moreover, CLSM analysis revealed that the biovolume and surface coverage of 49-old-biofilms grown on SilRef surfaces were lower than on EpoRef surfaces. These results can be explained by the foul release properties of this coating that prevent fouling settlements and provide extremely smooth and self-cleaning surfaces [8,10,11,15,48].

The properties of the fouling surfaces, together with the features of the fouling microorganisms, are the main factors that govern the fouling impact and strength of the biofouling interface [3]. The results demonstrated that the efficacy of SilRef-coated surfaces may be compromised by the microorganism.

Indeed, for *Cyanobium* sp. biofilms, the increase observed in all biofilm parameters was mainly due to the microorganism features. Accordingly, SilRef surfaces displayed higher activity against *P. tunicata* than *Cyanobium* sp. biofilms. For *Cyanobium* sp. biofilms formed on EpoRef surfaces, a combined effect between the surface and microorganism features played a considerable role in biofilm development at the maturation stage. The microfouler features also determined, to a lower extent, the biofilm formation. In addition, the properties of EpoRef surfaces contributed to a higher biofilm weight at the initial biofilm development stage. Lastly, the surface properties exerted a significant effect on *P. tunicata* biofilm development, contributing to a higher number of cells, wet weight, and thickness, especially in the biofilm maturation stage.

5. Conclusions

This work suggests that the dynamic behavior of biofilms developed on the different marine coatings is affected by the properties of the coatings, the microfoulers' features, and the interactions that are established between them in the different stages of biofilm development. Furthermore, it was shown that the SilRef marine coating is an effective, non-toxic commercial alternative to toxic biocide antifouling paints to control biofilm formation of common microfoulers.

Supplementary Materials: The following are available online at http://www.mdpi.com/2079-6412/10/9/893/s1, Figure S1: Representative images of water contact angle (θw) measurements on EpoRef (**a**) and SilRef (**b**) coatings.

Author Contributions: Conceptualization, S.I.F. and F.J.M.M.; Methodology, S.I.F. and L.C.G.; Formal analysis, S.I.F., R.T.-S., and L.C.G.; Investigation, S.I.F., R.T.-S., and L.C.G.; Resources, J.M., V.V., F.J.M.M., and E.R.S.; Data curation, S.I.F.; Writing—original draft preparation, S.I.F., R.T.-S., and L.C.G.; Writing—review and editing, R.T.-S., J.M., V.V., E.R.S., and F.J.M.M.; Supervision, F.J.M.M. All authors have read and agreed to the published version of the manuscript.

Funding: This research was funded by Base Funding—UIDB/00511/2020 of the Laboratory for Process Engineering, Environment, Biotechnology, and Energy—LEPABE—funded by national funds through the FCT/MCTES (PIDDAC), "CVMAR+i—Industrial Innovation and Marine Biotechnology Valorization" project, funded by INTERREG V Espanha Portugal (POCTEP) (0302_CVMAR_I_1_P), and UIDB/04423/2020 and UIDP/04423/2020 (CIIMAR). The research work was also supported by UIDB/04046/2020 and UIDP/04046/2020 research units grants, Portugal (to BioISI). R.T.-S. thanks the receipt of a junior researcher fellowship from the Project PTDC/BII-BIO/29589/2017—POCI-01-0145-FEDER-029589—funded by FEDER funds through COMPETE2020—Programa Operacional Competitividade e Internacionalização (POCI) and by national funds (PIDDAC) through FCT/MCTES. L.C.G. thanks the Portuguese Foundation for Science and Technology (FCT) for the financial support of her work contract through the Scientific Employment Stimulus-Individual Call-[CEECIND/01700/2017]. Atomic force microscopy technique was performed at the Biointerface and Nanotechnology i3S Scientific Platform with the assistance of Manuela Brás.

Conflicts of Interest: The authors declare no conflict of interest.

References

1. Tian, L.; Yin, Y.; Jin, H.; Bing, W.; Jin, E.; Zhao, J.; Ren, L. Novel marine antifouling coatings inspired by corals. *Mater. Today Chem.* **2020**, *17*, 100294. [CrossRef]
2. Silva, E.; Ferreira, O.; Ramalho, P.; Azevedo, N.; Bayón, R.; Igartua, A.; Bordado, J.; Calhorda, M. Eco-friendly non-biocide-release coatings for marine biofouling prevention. *Sci. Total Environ.* **2019**, *650*, 2499–2511. [CrossRef] [PubMed]
3. Kuliasha, C.A.; Fedderwitz, R.L.; Finlay, J.A.; Franco, S.C.; Clare, A.S.; Brennan, A.B. Engineered Chemical Nanotopographies: Reversible Addition–Fragmentation Chain-Transfer Mediated Grafting of Anisotropic Poly (acrylamide) Patterns on Poly (dimethylsiloxane) To Modulate Marine Biofouling. *Langmuir* **2019**, *36*, 379–387. [CrossRef]
4. Mineur, F.; Johnson, M.P.; Maggs, C.A.; Stegenga, H. Hull fouling on commercial ships as a vector of macroalgal introduction. *Mar. Biol.* **2007**, *151*, 1299–1307. [CrossRef]
5. Lacoursière-Roussel, A.; Forrest, B.M.; Guichard, F.; Piola, R.F.; McKindsey, C.W. Modeling biofouling from boat and source characteristics: A comparative study between Canada and New Zealand. *Biol. Invasions* **2012**, *14*, 2301–2314. [CrossRef]

6. Neves, A.R.; Almeida, J.R.; Carvalhal, F.; Câmara, A.; Pereira, S.; Antunes, J.; Vasconcelos, V.; Pinto, M.; Silva, E.R.; Sousa, E. Overcoming environmental problems of biocides: Synthetic bile acid derivatives as a sustainable alternative. *Ecotoxicol. Environ. Saf.* **2020**, *187*, 109812. [CrossRef]
7. Gu, J.-D. Microbial Biofilms, Fouling, Corrosion, and Biodeterioration of Materials. In *Handbook of Environmental Degradation of Materials*; Elsevier: Oxford, UK, 2018; pp. 273–298.
8. Selim, M.S.; Shenashen, M.; El-Safty, S.A.; Higazy, S.; Selim, M.M.; Isago, H.; Elmarakbi, A. Recent progress in marine foul-release polymeric nanocomposite coatings. *Prog. Mater. Sci.* **2017**, *87*, 1–32. [CrossRef]
9. Tu, C.; Chen, T.; Zhou, Q.; Liu, Y.; Wei, J.; Waniek, J.J.; Luo, Y. Biofilm formation and its influences on the properties of microplastics as affected by exposure time and depth in the seawater. *Sci. Total Environ.* **2020**, *734*, 139237. [CrossRef]
10. Hempel. *Product Data HEMPASIL X3+ 87500*; Hempel: Lyngby, Denmark, 2016.
11. Banerjee, I.; Pangule, R.C.; Kane, R.S. Antifouling coatings: Recent developments in the design of surfaces that prevent fouling by proteins, bacteria, and marine organisms. *Adv. Mater.* **2011**, *23*, 690–718. [CrossRef]
12. Hu, P.; Xie, Q.; Ma, C.; Zhang, G. Silicone-based fouling-release coatings for marine antifouling. *Langmuir* **2020**, *36*, 2170–2183. [CrossRef]
13. Krishnan, S.; Weinman, C.J.; Ober, C.K. Advances in polymers for anti-biofouling surfaces. *J. Mater. Chem.* **2008**, *18*, 3405–3413. [CrossRef]
14. Zhu, H.-W.; Zhang, J.-N.; Su, P.; Liu, T.; He, C.; Feng, D.; Wang, H. Strong adhesion of poly (vinyl alcohol)-glycerol hydrogels onto metal substrates for marine antifouling applications. *Soft Matter* **2020**, *16*, 709–717. [CrossRef] [PubMed]
15. Murosaki, T.; Ahmed, N.; Gong, J.P. Antifouling properties of hydrogels. *Sci. Technol. Adv. Mater.* **2012**. [CrossRef] [PubMed]
16. Chambers, L.D.; Stokes, K.R.; Walsh, F.C.; Wood, R.J. Modern approaches to marine antifouling coatings. *Surf. Coat. Technol.* **2006**, *201*, 3642–3652. [CrossRef]
17. Palmer, J.; Flint, S.; Brooks, J. Bacterial cell attachment, the beginning of a biofilm. *J. Ind. Microbiol. Biotechnol.* **2007**, *34*, 577–588. [CrossRef]
18. Mostafaei, A.; Nasirpouri, F. Preparation and characterization of a novel conducting nanocomposite blended with epoxy coating for antifouling and antibacterial applications. *J. Coat. Technol. Res.* **2013**, *10*, 679–694. [CrossRef]
19. Hoge, J.; Leach, C. Epoxy resin infused boat hulls. *Reinf. Plast.* **2016**, *60*, 221–223. [CrossRef]
20. Rao, D.; Webb, J.S.; Kjelleberg, S. Competitive interactions in mixed-species biofilms containing the marine bacterium *Pseudoalteromonas tunicata*. *Appl. Environ. Microbiol.* **2005**, *71*, 1729–1736. [CrossRef]
21. Abouelkheir, S.S.; Ghozlan, E.A.A.H.A.; Sabry, S.A. Characterization of Biofilm Forming Marine *Pseudoalteromonas* spp. *J. Mar. Sci.* **2020**, *2*. [CrossRef]
22. Komárek, J.; Anagnostidis, K. *Cyanoprokaryota, Part 1: Chroococcales*; Gustav Fischer Verlag: Stuttgart, Germany, 1998.
23. Faria, S.I.; Teixeira-Santos, R.; Romeu, M.J.; Morais, J.; Vasconcelos, V.; Mergulhão, F.J. The Relative Importance of Shear Forces and Surface Hydrophobicity on Biofilm Formation by Coccoid Cyanobacteria. *Polymers* **2020**, *12*, 653. [CrossRef]
24. Horcas, I.; Fernández, R.; Gomez-Rodriguez, J.; Colchero, J.; Gómez-Herrero, J.; Baro, A. WSXM: A software for scanning probe microscopy and a tool for nanotechnology. *Rev. Sci. Instrum.* **2007**, *78*, 013705. [CrossRef] [PubMed]
25. van Oss, C. *Interfacial Forces in Aqueous Media*; Marcel Dekker: New York, NY, USA, 1994.
26. Gomes, L.C.; Silva, L.N.; Simões, M.; Melo, L.F.; Mergulhão, F.J. Escherichia coli adhesion, biofilm development and antibiotic susceptibility on biomedical materials. *J. Biomed. Mater. Res. Part A* **2015**, *103*, 1414–1423. [CrossRef] [PubMed]
27. Lee, J.-W.; Nam, J.-H.; Kim, Y.-H.; Lee, K.-H.; Lee, D.-H. Bacterial communities in the initial stage of marine biofilm formation on artificial surfaces. *J. Microbiol.* **2008**, *46*, 174–182. [CrossRef] [PubMed]
28. Sekar, R.; Venugopalan, V.; Satpathy, K.; Nair, K.; Rao, V. Laboratory studies on adhesion of microalgae to hard substrates. In *Asian Pacific Phycology in the 21st Century: Prospects and Challenges*; Springer: Amsterdam, The Netherlands, 2004; pp. 109–116.
29. Holmström, C.; James, S.; Neilan, B.A.; White, D.C.; Kjelleberg, S. *Pseudoalteromonas tunicata* sp. nov., a bacterium that produces antifouling agents. *Int. J. Syst. Evol. Microbiol.* **1998**, *48*, 1205–1212. [CrossRef]

30. Ramos, V.; Morais, J.; Castelo-Branco, R.; Pinheiro, Â.; Martins, J.; Regueiras, A.; Pereira, A.L.; Lopes, V.R.; Frazão, B.; Gomes, D.; et al. Cyanobacterial diversity held in microbial biological resource centers as a biotechnological asset: The case study of the newly established LEGE culture collection. *J. Appl. Phycol.* **2018**, *30*, 1437–1451. [CrossRef]
31. Kotai, J. *Instructions for Preparation of Modified Nutrient Solution Z8 for AlgaeNorwegian*; Institute for Water Research: Oslo, Norway, 1972.
32. Romeu, M.J.; Alves, P.; Morais, J.; Miranda, J.M.; de Jong, E.D.; Sjollema, J.; Ramos, V.; Vasconcelos, V.; Mergulhão, F.J. Biofilm formation behaviour of marine filamentous cyanobacterial strains in controlled hydrodynamic conditions. *Environ. Microbiol.* **2019**, *21*, 4411–4424. [CrossRef]
33. Bakker, D.; Van der Plaats, A.; Verkerke, G.; Busscher, H.; Van Der Mei, H. Comparison of velocity profiles for different flow chamber designs used in studies of microbial adhesion to surfaces. *Appl. Environ. Microbiol.* **2003**, *69*, 6280–6287. [CrossRef]
34. Telegdi, J.; Trif, L.; Románszki, L. Smart anti-biofouling composite coatings for naval applications. In *Smart Composite Coatings and Membranes*; Elsevier: Amsterdam, The Netherlands, 2016; pp. 123–155.
35. Romeu, M.J.; Domínguez-Pérez, D.; Almeida, D.; Morais, J.; Campos, A.; Vasconcelos, V.; Mergulhão, F.J. Characterization of planktonic and biofilm cells from two filamentous cyanobacteria using a shotgun proteomic approach. *Biofouling* **2020**, *36*, 631–645. [CrossRef]
36. Heydorn, A.; Nielsen, A.T.; Hentzer, M.; Sternberg, C.; Givskov, M.; Ersbøll, B.K.; Molin, S. Quantification of biofilm structures by the novel computer program COMSTAT. *Microbiology* **2000**, *146*, 2395–2407. [CrossRef]
37. Schneider, C.A.; Rasband, W.S.; Eliceiri, K.W. NIH Image to ImageJ: 25 years of image analysis. *Nat. Methods* **2012**, *9*, 671–675. [CrossRef]
38. Fang, H.; Huang, L.; Zhao, H.; Cheng, W.; Chen, Y.; Fazeli, M.; Shang, Q. Biofilm Growth and the Impacts on Hydrodynamics. In *Mechanics of Bio-Sediment Transport*; Springer: Berlin/Heidelberg, Germany, 2020; pp. 153–208.
39. Ali, A.; Jamil, M.I.; Jiang, J.; Shoaib, M.; Amin, B.U.; Luo, S.; Zhan, X.; Chen, F.; Zhang, Q. An overview of controlled-biocide-release coating based on polymer resin for marine antifouling applications. *J. Polym. Res.* **2020**, *27*, 1–17. [CrossRef]
40. De-la-Pinta, I.; Cobos, M.; Ibarretxe, J.; Montoya, E.; Eraso, E.; Guraya, T.; Quindós, G. Effect of biomaterials hydrophobicity and roughness on biofilm development. *J. Mater. Sci. Mater. Med.* **2019**, *30*, 77. [CrossRef] [PubMed]
41. Ozkan, A.; Berberoglu, H. Cell to substratum and cell to cell interactions of microalgae. *Colloids Surf. B Biointerfaces* **2013**, *112*, 302–309. [CrossRef] [PubMed]
42. Moreira, J.M.R.; Gomes, L.C.; Whitehead, K.A.; Lynch, S.; Tetlow, L.A.; Mergulhão, F.J. Effect of surface conditioning with cellular extracts on *Escherichia coli* adhesion and initial biofilm formation. *Food Bioprod. Process.* **2017**, *104*, 1–12. [CrossRef]
43. Mazumder, S.; Falkinham, J.O., III; Dietrich, A.M.; Puri, I.K. Role of hydrophobicity in bacterial adherence to carbon nanostructures and biofilm formation. *Biofouling* **2010**, *26*, 333–339. [CrossRef]
44. Thomen, P.; Robert, J.; Monmeyran, A.; Bitbol, A.-F.; Douarche, C.; Henry, N. Bacterial biofilm under flow: First a physical struggle to stay, then a matter of breathing. *PLoS ONE* **2017**, *12*, e0175197. [CrossRef]
45. Di Martino, P. Extracellular polymeric substances, a key element in understanding biofilm phenotype. *AIMS Microbiol.* **2018**, *4*, 274. [CrossRef]
46. Vidakovic, L.; Singh, P.K.; Hartmann, R.; Nadell, C.D.; Drescher, K. Dynamic biofilm architecture confers individual and collective mechanisms of viral protection. *Nat. Microbiol.* **2018**, *3*, 26–31. [CrossRef]
47. Serra, D.O.; Richter, A.M.; Klauck, G.; Mika, F.; Hengge, R. Microanatomy at cellular resolution and spatial order of physiological differentiation in a bacterial biofilm. *MBio* **2013**, *4*. [CrossRef]
48. Gittens, J.E.; Smith, T.J.; Suleiman, R.; Akid, R. Current and emerging environmentally-friendly systems for fouling control in the marine environment. *Biotechnol. Adv.* **2013**, *31*, 1738–1753. [CrossRef]